Simultaneous cervical CT angiography from routine contrast-enhanced neck CT with multi-detector CT scanning

Mehmet Teksam, Sean O. Casey, Eduard Michel, Charles L. Truwit

M. Teksam (E), S. O. Casey, E. Michel, C. L. Truwit
From the Department of Radiology, University of Minnesota Medical School, Minneapolis, MN, USA

Computed tomographic angiography (CTA) is a technique that has evolved in a rapidly changing interplay of hardware and software advances. CT scan times are becoming ever shorter, now allowing imaging of larger segments of arterial anatomy during circulation of the intravenous bolus of contrast material. Multidetector (or multislice) CT is the most recent dramatic advance that has had a formidable impact on the style, quality, and efficiency of CT scanning. The new multidetector scanners, when used with thinner collimations, represent a generational advance in CT scanning technology. The greatest advance of multislice CT is in extending the quality and capacity of CT angiographic studies (1).

In this pictorial assay, we demonstrate the results of cervical CT angiography acquired as a byproduct during routine contrast-enhanced neck CT exams with a multi-detector array helical CT scanner in the preoperative evaluation of patients with neck pathologies. We predict that routine cross-sectional imaging protocols with "built in" availability such as CTA raw data may become routinely used in the neck and other parts of the body due to their versatility.

Technique

Acquisition Protocol
· Triphasic IV injection (antecubital vein) of nonionic contrast material
·50 ml immediately at arrival of patient (to allow for tumor enhancement), then
· 3 ml/sec for 70 ml via power injector, then
· 2 ml/sec for 30 ml via power injector
· Prescan delay: 30 seconds
· Scanning: Single helix with Quad multidetector array, 0.5 sec per tube rotation.
· Scanner: Somatom Plus 4 Volume Zoom CT (Siemens Medical Systems, Forcheim, Germany)
· Collimation: 1mm X 4
· Pitch: 4.0 (equivalent pitch on older helical scanners: 1, table speed 8 mm/sec)
· Parameters: 140 kVp, 220 mA
· Display field of view: 18 cm
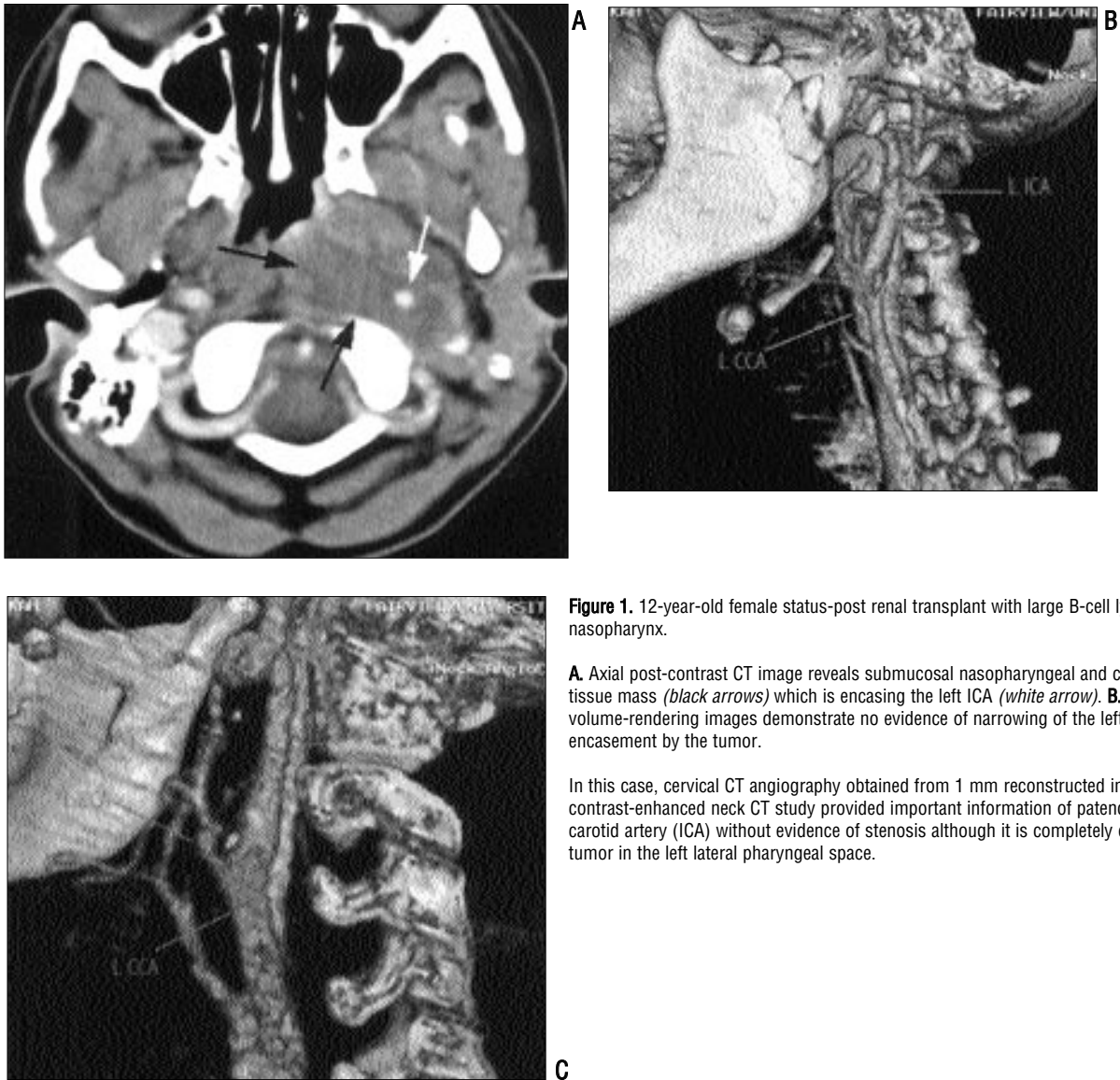· Coverage: From aortic arch to 1 cm above sella (including circle of Willis)

Figure 1. 12-year-old female status-post renal transplant with large B-cell lymphoma of nasopharynx.

A. Axial post-contrast CT image reveals submucosal nasopharyngeal and carotid space soft tissue mass *(black arrows)* which is encasing the left ICA *(white arrow)*. **B.** and **C.** Sagittal 3D volume-rendering images demonstrate no evidence of narrowing of the left ICA due to encasement by the tumor.

In this case, cervical CT angiography obtained from 1 mm reconstructed images of the routine contrast-enhanced neck CT study provided important information of patency of the left internal carotid artery (ICA) without evidence of stenosis although it is completely encased by the tumor in the left lateral pharyngeal space.

· Scan duration: 15-20 seconds

· Reconstructions:

Clinical neck CT images approximately 65 3mm thick sections

CTA raw data approximately 400 sections, 0.5 mm overlapping intervals

CT angiography source images and multiplanar reformations

Data sets (approximately 400 slices) were transferred to a Vital Images Vitrea Workstation (Vital Images Plymouth, MN USA) (Pentium III processor, Windows NT 4.0 operating system) for generation of 3-D CTA models if needed. Custom tailored neck presets on the Vitrea workstation allow virtually instantaneous access to source images, multiplanar (sagittal, coronal and oblique) reformations and a variety of 3D models. This advanced 3D workstation represents a generational advance in 3D rendering, allowing for virtually instantaneous interaction with the models as opposed to earlier methods recquiring cumbersome waits between almost every mouse click.

3D CT angiography display algorithms

The workstation allows quick switching among the maximum intensity projection (MIP) and 3D volume-rendering algorithms.

MIP: MIP is a 3D rendering technique that evaluates each voxel along a line from the viewer's eye through the volume of data and selects the maximum voxel value, which is then used as the displayed value. This display technique enables one to see high-density vessels through overlying soft tissues in the neck. Cutaway views can be used with MIP to eliminate overlapping bones. The so called "slab MIP" is also an effective viewing technique whereby MIP is applied to a smaller slab of the data which can then be slid back and forth interactively along an imaging plane through the larger data set.

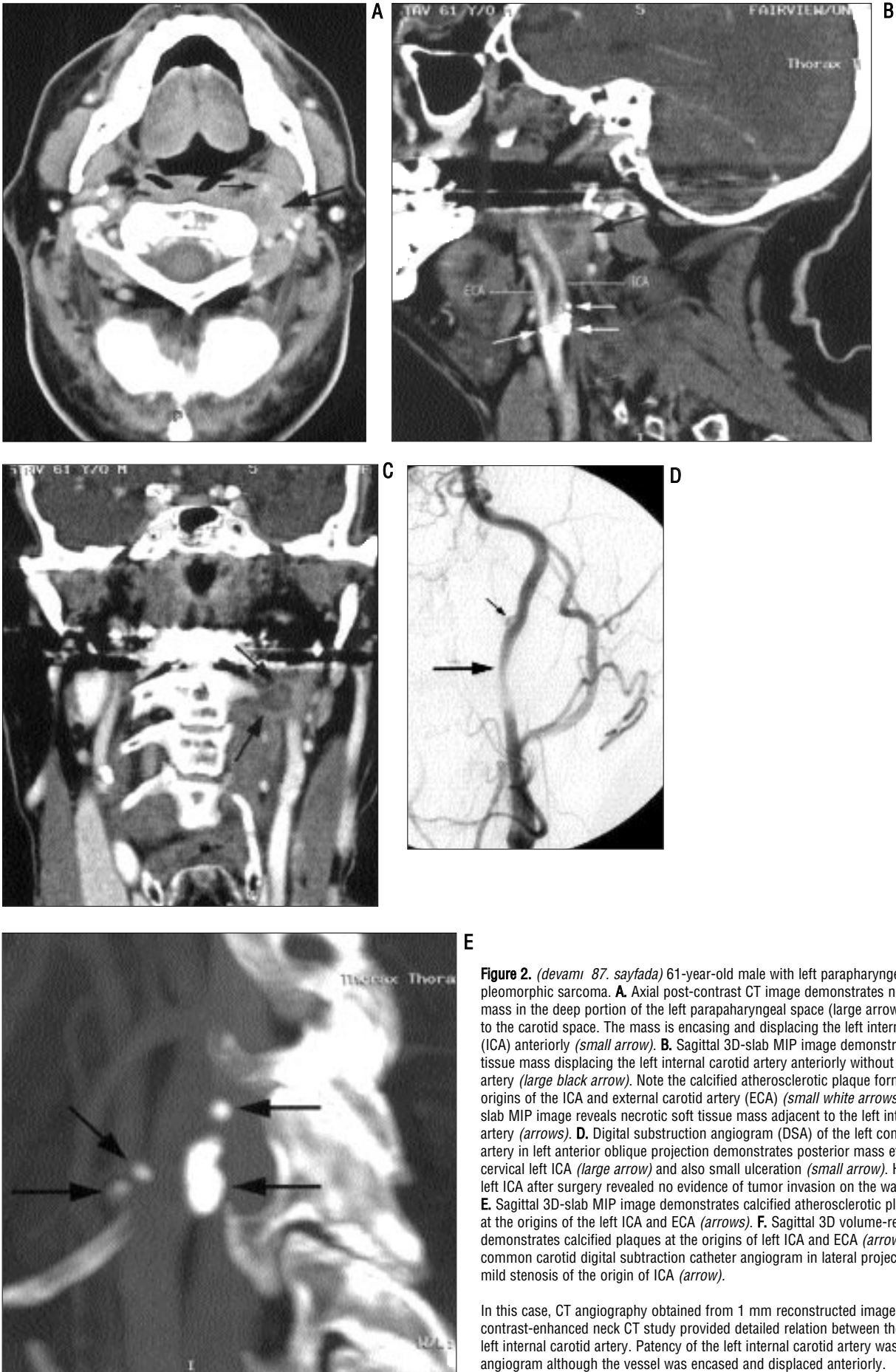MIP is the rendering algorithm which most closely resembles con-

Figure 2. *(devamı 87. sayfada)* 61-year-old male with left parapharyngeal high grade pleomorphic sarcoma. **A.** Axial post-contrast CT image demonstrates necrotic soft tissue mass in the deep portion of the left parapaharyngeal space (large arrow) which extends to the carotid space. The mass is encasing and displacing the left internal carotid artery (ICA) anteriorly *(small arrow)*. **B.** Sagittal 3D-slab MIP image demonstrates necrotic soft tissue mass displacing the left internal carotid artery anteriorly without narrowing of the artery *(large black arrow)*. Note the calcified atherosclerotic plaque formations at the origins of the ICA and external carotid artery (ECA) *(small white arrows)*. **C.** Coronal 3D-slab MIP image reveals necrotic soft tissue mass adjacent to the left internal carotid artery *(arrows)*. **D.** Digital substruction angiogram (DSA) of the left common carotid artery in left anterior oblique projection demonstrates posterior mass effect on the mid-cervical left ICA *(large arrow)* and also small ulceration *(small arrow)*. Histology of the left ICA after surgery revealed no evidence of tumor invasion on the wall of the vessel. **E.** Sagittal 3D-slab MIP image demonstrates calcified atherosclerotic plaque formations at the origins of the left ICA and ECA *(arrows)*. **F.** Sagittal 3D volume-rendering image demonstrates calcified plaques at the origins of left ICA and ECA *(arrows)*. **G.** Left common carotid digital subtraction catheter angiogram in lateral projection demonstrates mild stenosis of the origin of ICA *(arrow)*.

In this case, CT angiography obtained from 1 mm reconstructed images of the routine contrast-enhanced neck CT study provided detailed relation between the mass lesion and left internal carotid artery. Patency of the left internal carotid artery was seen on the CT angiogram although the vessel was encased and displaced anteriorly.
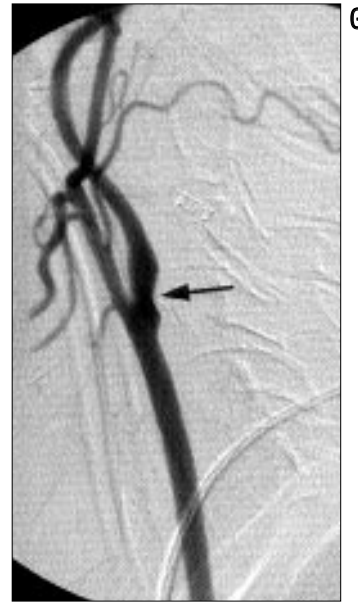
ventional catheter digital subtraction angiography. MIP, however, has a number of related artifacts and shortcomings that must be taken into account in order to interpret the rendered images properly (2). The displayed pixel intensity will represent only the material with the highest intensity along the projected array. A high intensity material such as calcification will obscure information from intravascular contrast material. This limitation can be partially overcome through volume editing.

3D Volume Rendering: 3D volume-rendering takes the entire volume of data, sums the contributions of each voxel along a line from the viewer's eye through the data set, and displays the resulting composite for each pixel of the display. Rendering parameters, which assign variable opacities and colors to differing density values, are applied to the full volume data set and affect the appearance of the image to be displayed. The window width and level functions are similar to windowing parameter settings on standard CT scanners or workstations. Significant levels of accuracy are achievable with volume rendering and thus 3D volume-rendering has some potential advantages over other rendering techniques (2).

Advantages of CT angiography

While catheter angiography has traditionally been considered the gold standard for carotid artery imaging, its associated cost and increased risk has prompted the development of other imaging techniques. Noninvasive imaging of extracranial carotid disease using duplex scan and magnetic resonance angiography (MRA) has become standard in the preoperative evaluation of carotid artery stenosis. However, these studies sometimes fail to differentiate between high-grade stenosis and total occlusion and often suffer from motion. In addition, dense calcified plaques can cause image artifact, making accurate measurement of carotid disease difficult.

Helical CT angiography is a safe, relatively noninvasive, rapidly evolving technique that allows the rapid acquisition of data which can be reconstructed into two- and three-dimensional images. MIP technique allows data to be reconstructed into images that closely resemble conventional angiograms and can be rotated to be viewed from any angle after the patient's examination (Figure 1,2).

The guidelines established by the recent cooperative studies on carotid endarterectomy in the treatment of pa-

tients with severe carotid artery stenosis depend on accurate determination of stenosis (3). This has prompted a renewed interest in the best and safest method of imaging the carotid bifurcation. Traditionally, catheter angiography has been considered the standard for measuring carotid artery stenosis. However, significant discrepancies in the angiographic criteria used in the North American Carotid Endarterectomy Trial (NASCET) and the European Carotid Surgery Trial (ECST) has resulted in continued controversy about the most accurate method of measuring carotid artery stenosis (4,5). The difficulty with both the NASCET and ECST methods lies in establishing the true diameter of the 'normal' internal carotid artery distal to the stenosis (NASCET), or the 'true' diameter of the vessel at the point of maximal stenosis (ECST). Both methods are subject to errors, because measurements are extrapolated based on an estimation of what is thought to be normal anatomy. In addition, because conventional non-3D catheter arteriography provides only static planar views, eccentricities of the vascular lumen may not be identified.

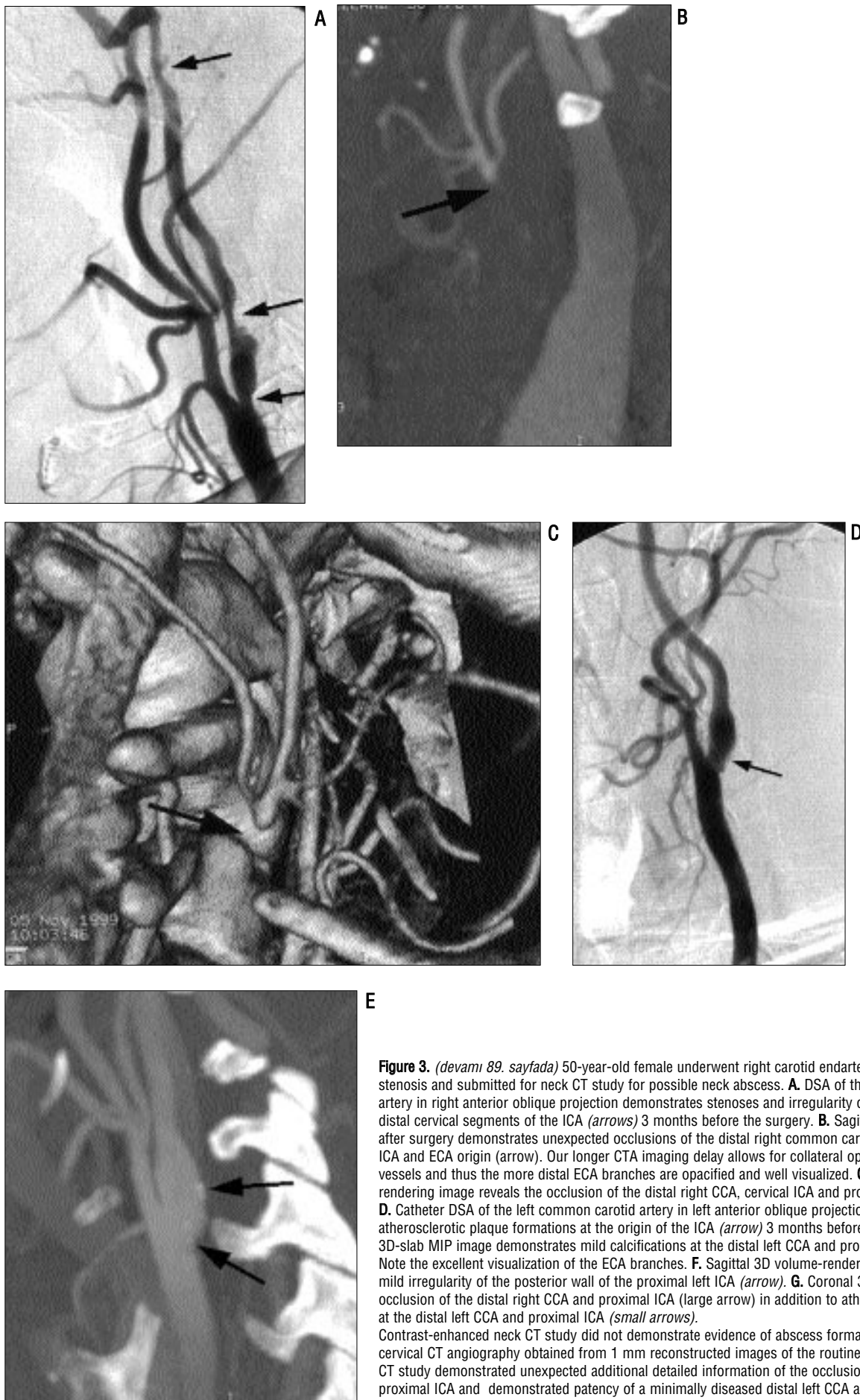Helical CT angiography, especially with the use of multislice CT scanner,

Figure 3. *(devamı 89. sayfada)* 50-year-old female underwent right carotid endarterectomy for high grade stenosis and submitted for neck CT study for possible neck abscess. **A.** DSA of the right common carotid artery in right anterior oblique projection demonstrates stenoses and irregularity of the origin, proximal and distal cervical segments of the ICA *(arrows)* 3 months before the surgery. **B.** Sagittal 3D-slab MIP image after surgery demonstrates unexpected occlusions of the distal right common carotid artery (CCA), cervical ICA and ECA origin (arrow). Our longer CTA imaging delay allows for collateral opacification of all patent vessels and thus the more distal ECA branches are opacified and well visualized. **C.** Sagittal 3D volume-rendering image reveals the occlusion of the distal right CCA, cervical ICA and proximal ECA *(arrow)*.
D. Catheter DSA of the left common carotid artery in left anterior oblique projection demonstrated mild atherosclerotic plaque formations at the origin of the ICA *(arrow)* 3 months before the surgery. **E.** Sagittal 3D-slab MIP image demonstrates mild calcifications at the distal left CCA and proximal left ICA *(arrows)*. Note the excellent visualization of the ECA branches. **F.** Sagittal 3D volume-rendering image demonstrates mild irregularity of the posterior wall of the proximal left ICA *(arrow)*. **G.** Coronal 3D-slab MIP image reveals occlusion of the distal right CCA and proximal ICA (large arrow) in addition to atherosclerotic calcifications at the distal left CCA and proximal ICA *(small arrows)*.

Contrast-enhanced neck CT study did not demonstrate evidence of abscess formation in the neck. However, cervical CT angiography obtained from 1 mm reconstructed images of the routine contrast-enhanced neck CT study demonstrated unexpected additional detailed information of the occlusion of the right CCA and proximal ICA and demonstrated patency of a minimally diseased distal left CCA and proximal ICA.
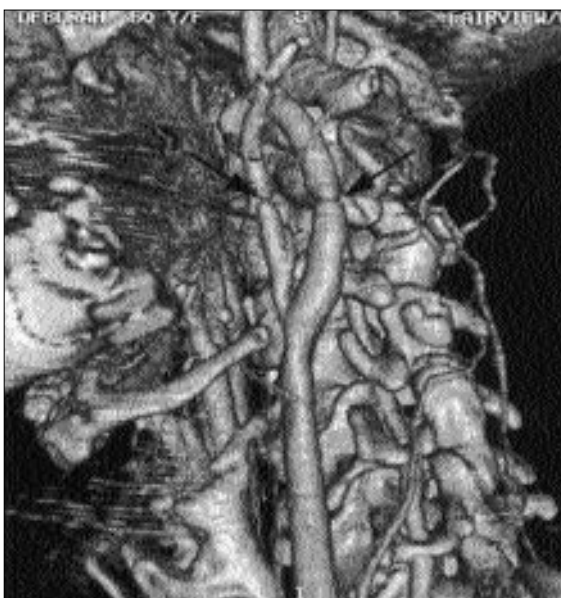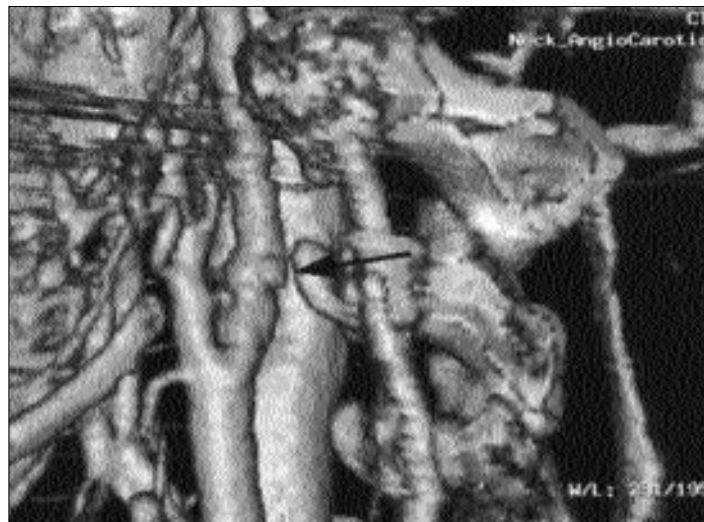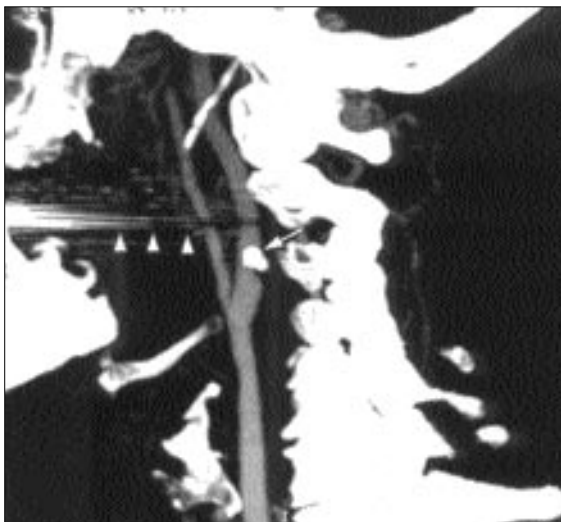
Figure 4. 50-year-old female with moderately differentiated squamous cell carcinoma of the soft palate on the left side of the neck. **A.** Sagittal 3D-slab MIP image demonstrate no significant stenosis of the carotid arteries. Large calcified plaque, however, is seen in the proximal left ICA *(arrow)*. Dental amalgam streak artifact mildly obscures the small segments of the vascular structures *(arrowheads)*. **B.** Sagittal 3D volume-rendering image demonstrates calcification on the posterior wall of the left ICA *(arrow)*. **C.** Sagittal 3D volume-rendering image demonstrates pseudo-stenotic appearance of the carotid arteries due to metallic artifacts from the teeth *(arrows)*. This is an example of the potential pitfall of the CT-angiography.
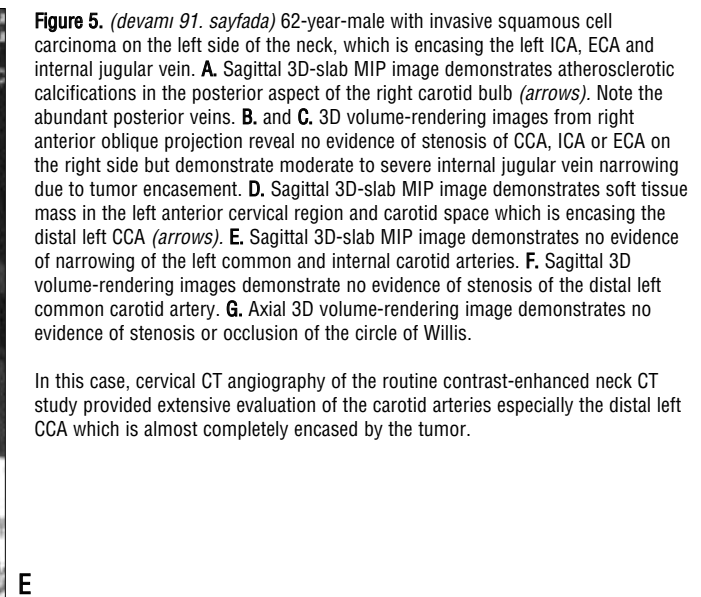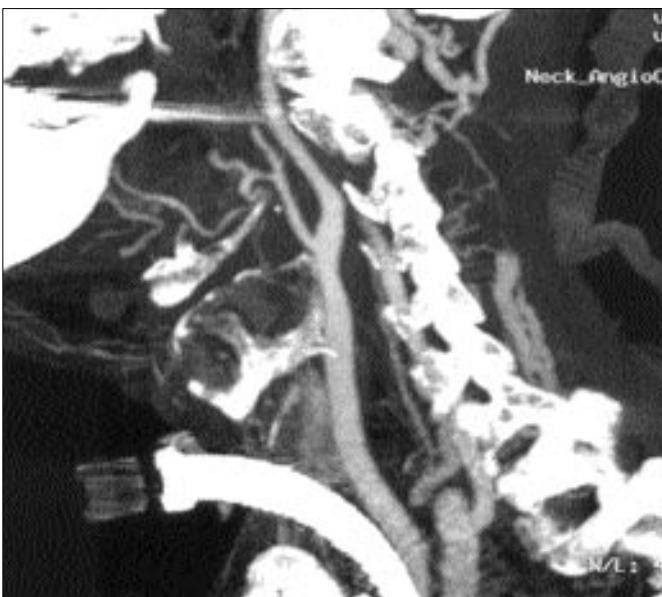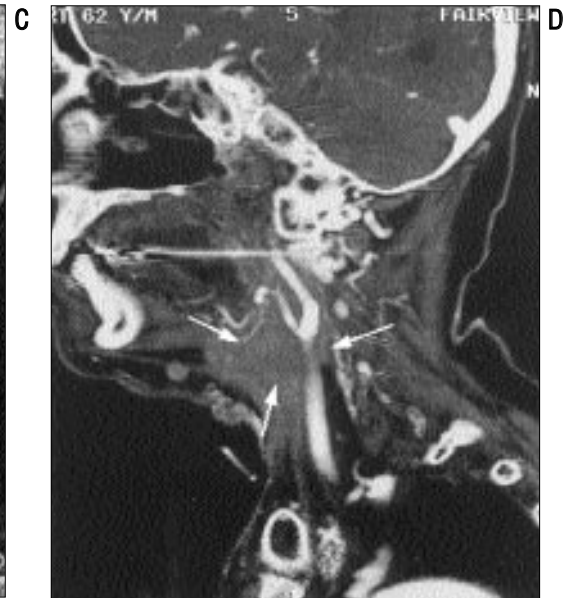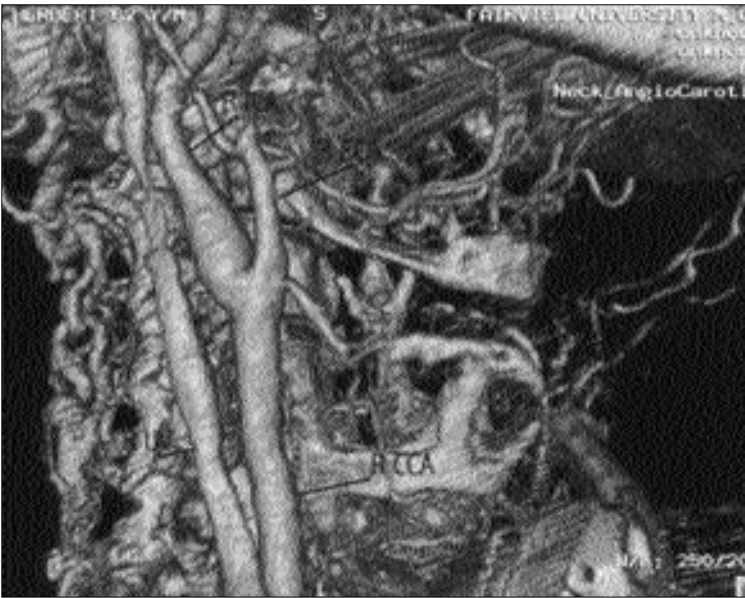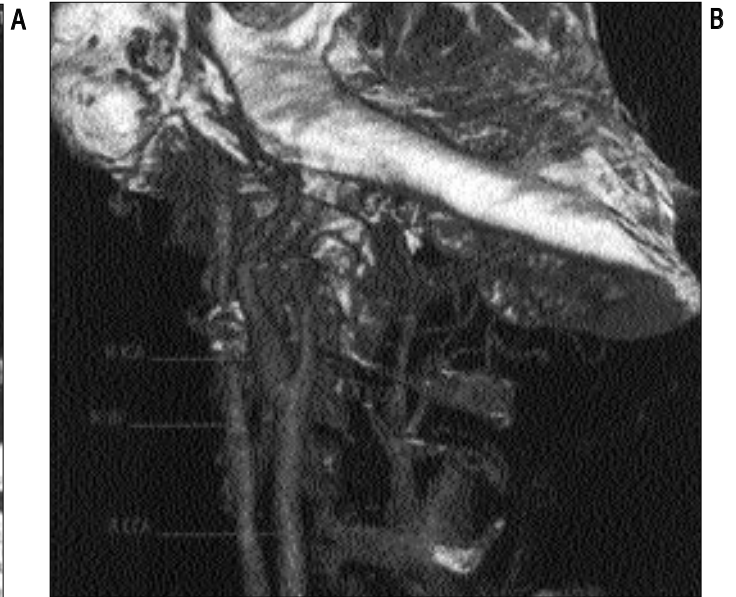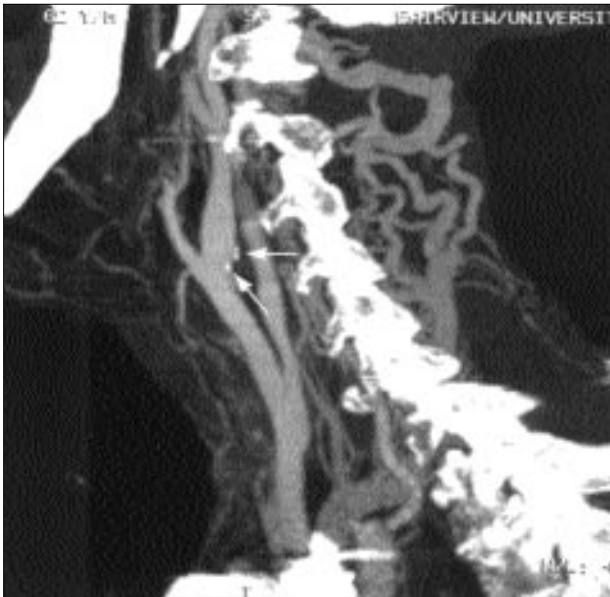
Figure 5. *(devamı 91. sayfada)* 62-year-male with invasive squamous cell carcinoma on the left side of the neck, which is encasing the left ICA, ECA and internal jugular vein. **A.** Sagittal 3D-slab MIP image demonstrates atherosclerotic calcifications in the posterior aspect of the right carotid bulb *(arrows)*. Note the abundant posterior veins. **B.** and **C.** 3D volume-rendering images from right anterior oblique projection reveal no evidence of stenosis of CCA, ICA or ECA on the right side but demonstrate moderate to severe internal jugular vein narrowing due to tumor encasement. **D.** Sagittal 3D-slab MIP image demonstrates soft tissue mass in the left anterior cervical region and carotid space which is encasing the distal left CCA *(arrows)*. **E.** Sagittal 3D-slab MIP image demonstrates no evidence of narrowing of the left common and internal carotid arteries. **F.** Sagittal 3D volume-rendering images demonstrate no evidence of stenosis of the distal left common carotid artery. **G.** Axial 3D volume-rendering image demonstrates no evidence of stenosis or occlusion of the circle of Willis.

In this case, cervical CT angiography of the routine contrast-enhanced neck CT study provided extensive evaluation of the carotid arteries especially the distal left CCA which is almost completely encased by the tumor.

F

G
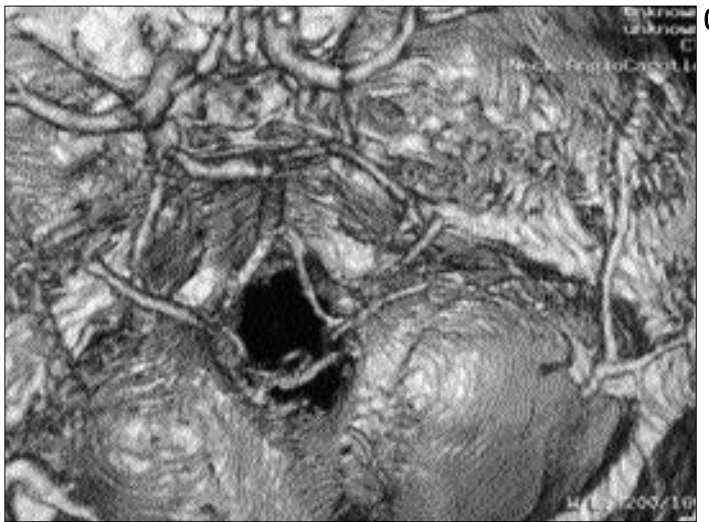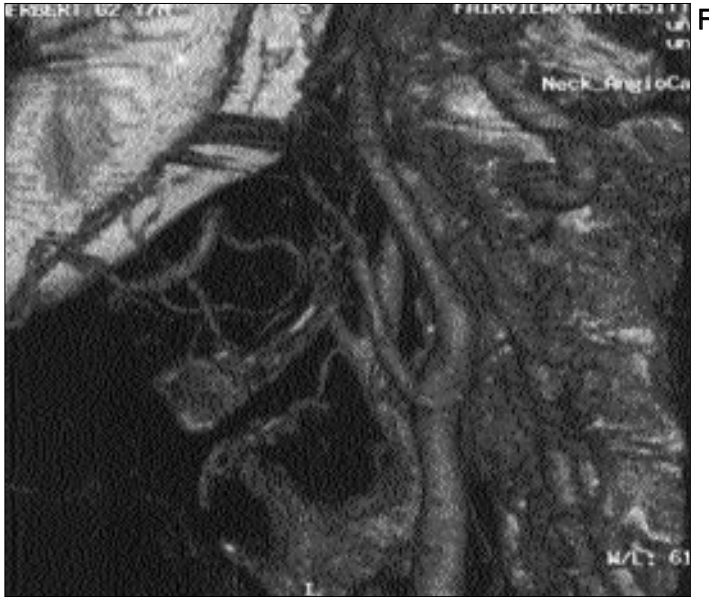
overcomes these drawbacks. CTA however has previously been limited by Z-axis resolution. Now with nearly isotropic voxels of multidetector scanning, inplane and Z-axis resolution are the remaining, although minor, limitations. Earlier CTA protocols had difficulty with timing and if insufficient scanning delay after contrast injection was used, the ability to detect the highest grade stenoses or so-called carotid "string signs" was less than optimal. We now use faster scanning at a longer delay, essentially imaging the equilibrium state. The only drawback

of this approach is overlap of enhancing veins, typically the internal jugular veins in close proximity to the carotid arteries. Although 3D images are useful for review with clinicians to provide an angiographic-like view, we prefer performing stenosis measurements by applying NASCET criteria to the cross-sectional diameter of the abnormal and normal portions of the vessel (in an axial or oblique plane perpendicular to the measured arterial segment). Other advantages of CT angiography are rapid data acquisition and lack of flow-related artifacts (as

compared with non-contrast MRA). The main disadvantages of CT angiography still include the need to use IV contrast and metallic dental artifacts.

Facial trauma and head and neck oncologic patients are often destined for extensive reconstructive procedures with microvascular free flaps due to ablative injuries or postoperative defects. The integrity and competence of the vasculature in the head and neck recipient site must be imaged and evaluated preoperatively as an essential prerequisite for the success of the reconstructive transfer. In patients with ICA tumor encasement, CTA can provide vascular imaging competitive with angiography (Figure 3-5). However, many of these patients will still require catheter angiography for balloon test occlusion procedures in order to acquire functional and clinical measures of the patient's ability to tolerate vascular sacrifice. Although the ability to perform these 3D CTA reconstructions is present in every multidetector CT of the neck, in the interest of efficiency, we generally reserve reference to these data sets to those patients with abnormalities seen on the standard axial images. Nevertheless, some benefit appears to exist from the occasional use of this "free" CTA data within the raw neck CT data. In selected patients, the availability of these CTA reconstructions may spare the patient the need for catheter angiography.

Conclusion

High quality CT angiography of the neck obtained simultaneously during the acquisition of the routine contrast-enhanced CT study of the neck, utilizing the multi-detector array helical CT scanner provides additional information in surgical planning of some patients with neck pathologies. The protocol appears to be technically robust.

References

1. Tanenbaum LN. Thin slices improve view of CNS structures. Diagnostic Imaging 1999; 11:10-12 .
2. Calhoun PS, Kuszyk BS, Heath DG, Carley JC, Fishman EK. Three-dimensional rendering of spiral CT data: theory and method. Radiographics 1999; 19:745-764.
3. Barnett HJM, Taylor DW, Haynes RB, et al. Beneficial effect of carotid endarterectomy in symptomatic patients with high-grade carotid stenosis. N Engl J Med 1991; 325:445-453.
4. Fox AJ. How to measure carotid stenosis. Radiology 1993; 186:316-318.
5. Hobson RW, Strandness DE. Carotid artery stenosis: What's in the measurement? J Vasc Surg 1993; 18:1069-70.